EMBO reports

scientific report

Nuclear movement during myotube formation is microtubule and dynein dependent and is regulated by Cdc42, Par6 and Par3

Bruno Cadot[1,2], Vincent Gache[1,2*], Elena Vasyutina[3], Sestina Falcone[1,2], Carmen Birchmeier[3] & Edgar R. Gomes[1,2+]*

[1]UMR S 787 INSERM, Université Pierre et Marie Curie Paris 6, [2]Groupe Hospitalier Pitié-Salpêtrière, Institut de Myologie, Paris, France, and [3]Department of Neuroscience, Max-Delbruck-Centrum for Molecular Medicine, Berlin, Germany

Cells actively position their nucleus within the cytoplasm. One striking example is observed during skeletal myogenesis. Differentiated myoblasts fuse to form a multinucleated myotube with nuclei positioned in the centre of the syncytium by an unknown mechanism. Here, we describe that the nucleus of a myoblast moves rapidly after fusion towards the central myotube nuclei. This movement is driven by microtubules and dynein/dynactin complex, and requires Cdc42, Par6 and Par3. We found that Par6β and dynactin accumulate at the nuclear envelope of differentiated myoblasts and myotubes, and this accumulation is dependent on Par6 and Par3 proteins but not on microtubules. These results suggest a mechanism where nuclear movement after fusion is driven by microtubules that emanate from one nucleus that are pulled by dynein/dynactin complex anchored to the nuclear envelope of another nucleus.

Keywords: nuclear movement; microtubules; skeletal muscle; Par6; dynein

EMBO *reports* (2012) **13,** 741–749. doi:10.1038/embor.2012.89

INTRODUCTION

Nuclear positioning within cells is required for zygote formation, mitosis, cell migration and multiple developmental processes. Abnormal nuclear positioning is associated with muscle and brain pathologies [1]. Nuclear movement events are mainly driven by microtubules (MTs) and actin cytoskeletons [2,3].

The small GTPase Cdc42 is a major regulator of the cytoskeleton and cell polarization, and regulates multiple nuclear positioning events [4,5]. One Cdc42 effector, Par6, is part of a conserved complex involved in cell polarization. Par6 forms a complex with Par3, via the PDZ domains [6], and controls cytoskeleton organization during spindle positioning, apical–basal epithelia formation and neuronal polarization [7,8]. Par proteins have been implicated in nuclear movement in Drosophila oocyte [9]. However, a role for Par proteins in nuclear movement in vertebrates has not been established.

An extreme example of nuclear positioning occurs in skeletal muscle. During muscle formation, multinucleated myotubes are generated by the fusion of differentiated myoblasts, which then differentiate into myofibers. Myotubes are characterized by centrally located nuclei while myofiber nuclei are positioned in the periphery, with few nuclei specifically clustered at the neuromuscular junction [10]. These observations suggest that multiple nuclear movements occur during myofiber formation. Classic time-lapse microscopy studies showed that nuclei move within the centre of myotubes but it is not known how the myoblast nucleus reaches the centre of the myotube after fusion [11]. The position of nuclei in muscle fibres has been used as a diagnostic tool for more than 40 years to identify multiple muscle disorders [12], and it is not clear if mispositioned nuclei lead to muscle disorders. We recently demonstrate that improper nuclear positioning affects muscle function, suggesting that mispositioned nuclei in muscle disorders might be involved in the pathology [13].

The MT network is dramatically reorganized during myotube formation. In nondifferentiated myoblasts, MTs nucleate and are anchored to the centrosome whereas in differentiated myoblasts and myotubes, the nuclear envelope (NE) accumulates centrosomal proteins, such as pericentrin, and becomes the main MT organizing centre [14]. In multinucleated myotubes, most of the MTs remain attached to the NE and form long parallel arrays throughout the myotube [14–16].

Here we show that after fusion, the nucleus of the myoblast moves towards the centre of the myotubes driven by MTs and dynein/dynactin complex, and this process is regulated by Cdc42, Par6 and Par3.

[1]UMR S 787 INSERM, Université Pierre et Marie Curie Paris 6, Paris 75634, France
[2]Groupe Hospitalier Pitié-Salpêtrière, Institut de Myologie, Paris 75013, France
[3]Department of Neuroscience, Max-Delbruck-Centrum for Molecular Medicine, Robert-Roessle-Strasse 10, Berlin 13125, Germany
*These authors contributed equally to this work
+Corresponding author. Tel: +33 66 078 3363; Fax: +33 15 360 0802;
E-mail: edgar.gomes@upmc.fr

Received 2 January 2012; revised 4 May 2012; accepted 21 May 2012; published online 26 June 2012

Fig 1 | Nuclear movement after fusion requires MTs. (**A**) Frames from a time-lapse two-channel movie (phase contrast and fluorescence) of differentiated GFP-H1-C2 myoblasts during fusion (supplementary Movie S2 online). A myoblast (red outline) fused with a myotube (green outline) to form a new myotube (white outline; time in h:min). Note that after fusion (0:40), myoblast nucleus (arrowhead) moves towards the myotube nuclei (arrow). (**B**) Frames from a time-lapse movie of differentiated primary myoblasts during fusion (supplementary Movie S3 online). A myoblast (red outline) fused with a myotube (green outline) to form a new myotubes (white outline). Note that after fusion (00:40) myoblast nucleus (arrowhead) moves towards the myotube nuclei (arrow). (**C**) Speed of the nuclei after fusion of myoblasts into myotubes on differentiated GFP-H1-C2 and primary myoblasts. (**D**) Plot representing the distance between the myoblast nucleus and the nuclei in the centre of the myotube (distance between nuclei, *y* axis) and the time delay between fusion and initiation of myoblast nuclear movement (delay before nuclear movement, *x* axis). (**E**) Frames from a time-lapse two-channel movie of differentiated GFP-H1-C2 myoblasts during fusion of a myoblast (red outline) with a myotube (green outline) after addition of 100 nM taxol (supplementary Movie S4 online). Fusion occurred between 00:15 and 00:30, and taxol was added at 00:45. Note that myoblast nucleus (arrowhead) did not move towards the myotube nuclei (arrow). (**F**) Speed of the nuclei after fusion of differentiated GFP-H1-C2 cells in nontreated, non-transfected myotubes (Ctr), myotubes expressing the indicated spastin constructs as in supplementary Fig S1a online, or myotubes treated with 75 nM nocodazole (Ndz) or 100 nM taxol as in (**E**). Scale bar in (**A,B,E**), 20 μm. *P*-value in (**C,D,F**); $^{**}P<0.01$, $^{***}P<0.005$. Red line indicates the median. MTs, microtubules.

RESULTS AND DISCUSSION

Microtubules drive nuclear movement after fusion

To study how the nucleus of myoblasts reach the centre of the myotube after fusion, we used C2C12 myogenic cell line expressing stably green fluorescent protein (GFP)-histone H1 that can be differentiated into myotubes upon switching to differentiation media (DM). We followed nuclear movement during myotube differentiation using multipositioning time-lapse microscopy (supplementary Movie S1 online). When a myoblast fused at the distal end of a myotube (which occurred in more than 60% of the observed events fusions), the newly fused myoblast nucleus moved towards the centre of the myotube nuclei right after fusion (16.7 ± 2.3 min, $n = 149$) at a speed of 0.76 μm/min (Fig 1A,C; supplementary Movie S2 online). The same general properties were also found using primary myoblasts from newborn mouse muscles, and the nuclear movement after fusion speed was 0.88 μm/min (Fig 1B,C; supplementary Movie S3 online). Interestingly, we observed a bigger delay between fusion and initiation of nuclear movement in situations where the distance between the myoblast nucleus and the nuclei in the centre of the myotube was higher, suggesting an interplay between these nuclei (Fig 1D).

Next, we investigated the role of MTs in nuclear movement by overexpression of spastin, a MT severing protein, either in myoblasts or myotubes [17] (supplementary Fig S1a online). We found that overexpression of spastin, but not of nonsevering spastin mutant (E442Q-spastin), in myotubes dramatically reduces nuclear movement after fusion of nonexpressing myoblast (Fig 1F). We never observed fusion of spastin-expressing myoblasts.

To test the role of MTs dynamics on nuclear movement, we used taxol (a MT-stabilizing drug) and nocodazole (a MT-depolymerizing drug) at very low concentrations known to impair MT dynamics [18,19] and found that fusion was inhibited (data not shown), preventing the analysis of nuclear movement that occurs after fusion. To overcome this problem, we added the inhibitors right after a fusion event and before nuclear movement had occurred. As yet, we have not been able to predict fusion events and these occur on an average of 2.7 ± 0.16 events per myotube in 24 h. To circumvent the low rate of fusion per myotube, we performed multipositioning time-lapse imaging of differentiating myotubes before and after the addition of the inhibitor, and analysed only the fusion events that occurred no more than 15 min before inhibitor addition. We found that nuclear movement after fusion was inhibited in the presence of taxol or nocodazol (Fig 1E,F; supplementary Movie S4 online). Thus, MTs dynamics are required for nuclear movements after myoblast fusion.

Dynein and dynactin are involved in nuclear movement

The dynein/dynactin complex drives MT-dependent organelle movement [20,21]. We found that nuclear movement after fusion was reduced in dynein heavy chain (DHC), dynein intermediate chain (IC2) or dynactin p150 subunit (p150) short interfering RNA (siRNA)-treated GFP-H1-C2 and primary cells (Fig 2A,B; supplementary Fig S1b online, supplementary Movie S5 online) without any effect on fusion index or MT organization (supplementary Figs S1d and S5a,b online). Overexpression of p50 subunit of dynactin in myotubes that inhibits dynein/dynactin complex also reduced nuclear movement after fusion of non-expressing myoblasts (Fig 2A; supplementary Fig S1c online, supplementary Movie S6 online). Therefore dynein/dynactin complex is involved in nuclear movement after fusion.

Cdc42, Par6 and Par3 regulate nuclear movement

We investigated the role of the small G-protein Cdc42 in nuclear movement after myoblast fusion. As Cdc42 is involved in myotubes fusion (supplementary Fig S1d online) [22], we used primary myoblasts from *Cdc42* flox mice [23]. In the absence of Cre recombinase, Cdc42 is expressed and cells fuse, form myotubes and nuclei move after fusion at the same speed as wild-type myoblasts (Fig 2C–E). After infection with an adenovirus encoding Cre recombinase after transfer to DM, Cdc42 levels are decreased without affecting fusion index (supplementary Fig S1e,f online) and nuclear movement after fusion is reduced when compared with uninfected cells (Fig 2C–E; supplementary Movies S7 and S8 online). In addition, microinjection of dominant-negative (Cdc42N17) and constitutively active (Cdc42V12) GFP-Cdc42 [24] in myotubes reduced nuclear movement after fusion, although we observed very few fusion events (Cdc42N17, $n = 3$ and Cdc42V12, $n = 4$; Fig 2F), as previously described [22,23]. Overall, these results demonstrate that Cdc42 is required for nuclear movement after fusion.

Par6 is a Cdc42 effector involved in cell polarization that interacts with Par3 and regulates dynein-dependent MT polarity [4,25,26]. We investigated the role of Par3 and the three mammalian *Par6* genes (α, β and γ), which may have distinct functions [27], on nuclear movement after fusion. Depletion of

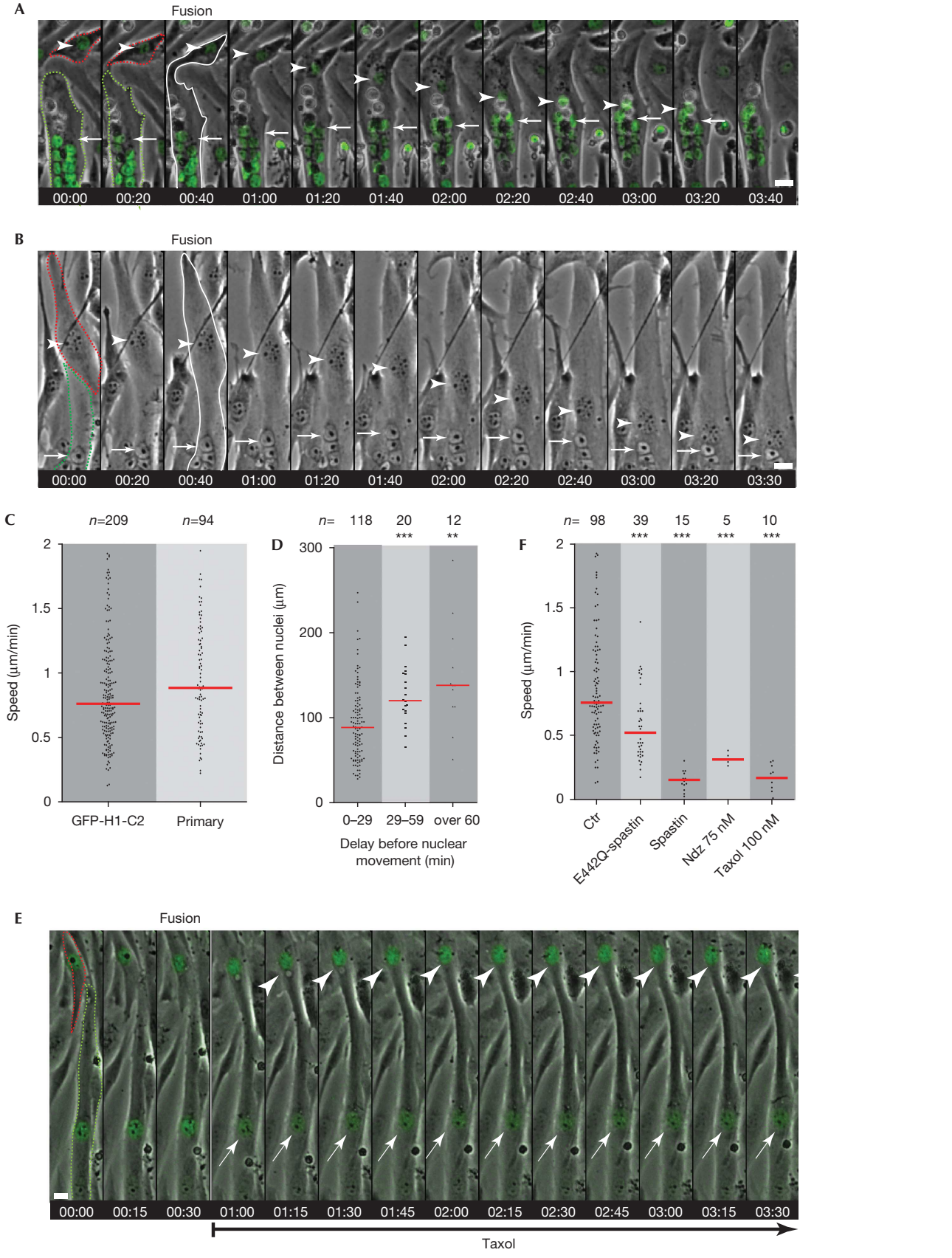
A
Fusion
00:00
00:20
00:40
01:00
01:20
01:40
02:00
02:20
02:40
03:00
03:20
03:40
B
Fusion
00:00
00:20
00:40
01:00
01:20
01:40
02:00
02:20
02:40
03:00
03:20
03:30
C
n=209
n=94
Speed (µm/min)
2
1.5
1
0.5
0
GFP-H1-C2
Primary
D
n= 118 20 12
***
**
Distance between nuclei (µm)
300
200
100
0
0–29
29–59
over 60
Delay before nuclear movement (min)
F
n= 98 39 15 5 10
***
***
***
***
Speed (µm/min)
2
1.5
1
0.5
0
Ctr
E442Q-spastin
Spastin
Ndz 75 nM
Taxol 100 nM
E
Fusion
00:00
00:15
00:30
01:00
01:15
01:30
01:45
02:00
02:15
02:30
02:45
03:00
03:15
03:30
Taxol

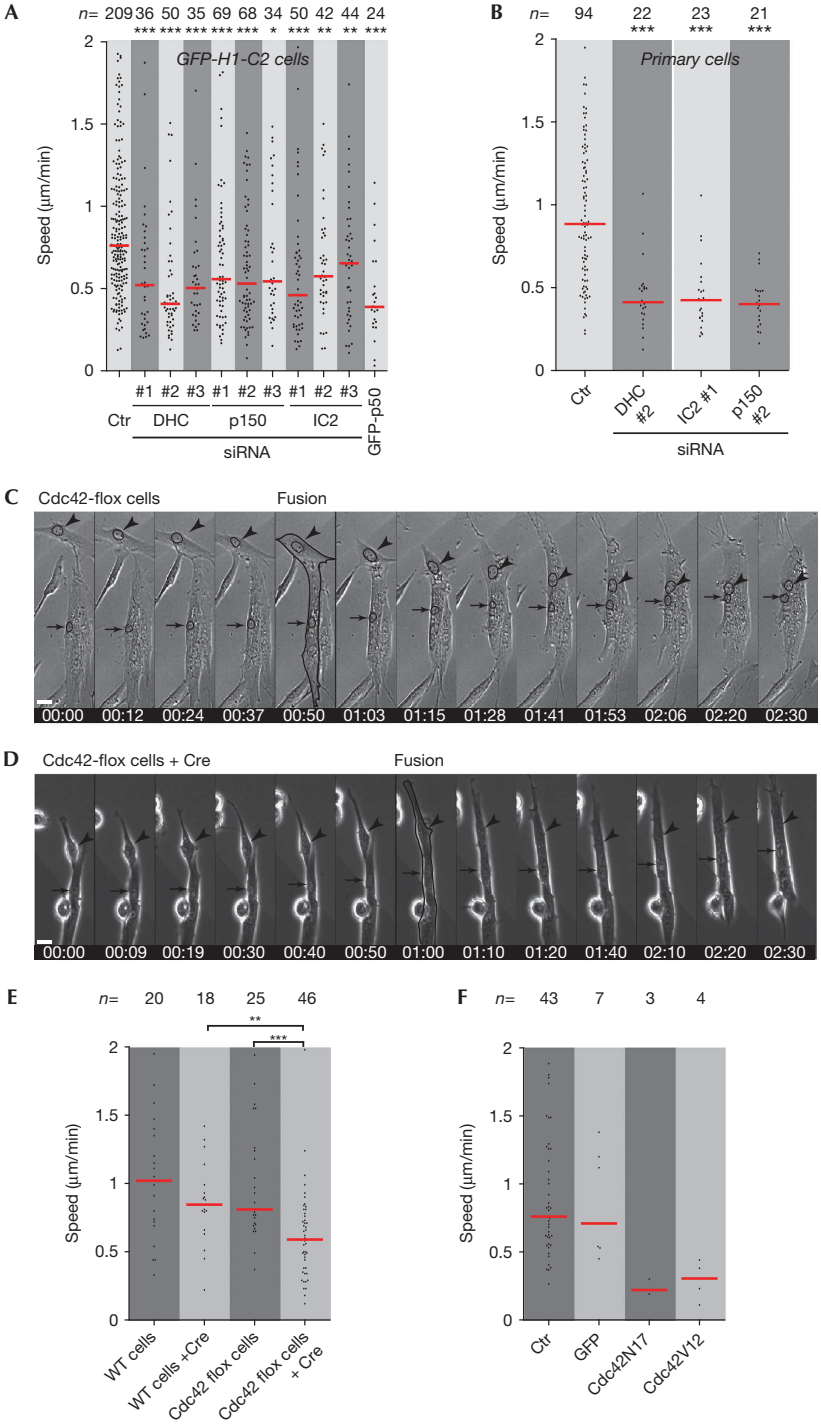

Fig 2 | Cdc42 regulates nuclear movement after fusion. (**A**) Speed of the nuclei after fusion of differentiated GFP-H1-C2 cells in nontreated, treated with three different siRNA against DHC, IC2, p150 or myotubes transfected with GFP-p50. (**B**) Speed of the nuclei after fusion of differentiated primary myoblasts in untreated or after transfection with the indicated siRNAs. (**C,D**) Frames from a time-lapse movie of differentiated primary myoblasts isolated from Cdc42 flox mice (supplementary Movies S5 and S6 online). A myoblast (arrowhead) fused with a myotube (arrow) to form a new myotubes (black outline) in the absence (**C**) or presence (**D**) of a Cre-encoding adenovirus. The myoblast nucleus and the myotube nuclei are highlighted by a black circle in (**C**). Note that in Cre-treated cultures, nuclear movement after fusion was reduced. Scale Bar, 20 µm. (**E**) Speed of the nuclei after fusion in WT primary cells or primary Cdc42 flox myoblasts in the absence or presence of Cre-encoding adenovirus. (**F**) Speed of the nuclei after fusion of differentiated GFP-H1-C2 cells in myotubes nonmicroinjected or microinjected with constructs encoding GFP, Cdc42N17 or Cdc42V12. *P*-value in (**A**), (**B**), (**E**) and (**F**); $*P<0.05$, $**P<0.01$, $***P<0.005$. Red line indicates the median. DHC, dynein heavy chain; GFP, green fluorescent protein; siRNA, short interfering RNA; WT, wild-type.

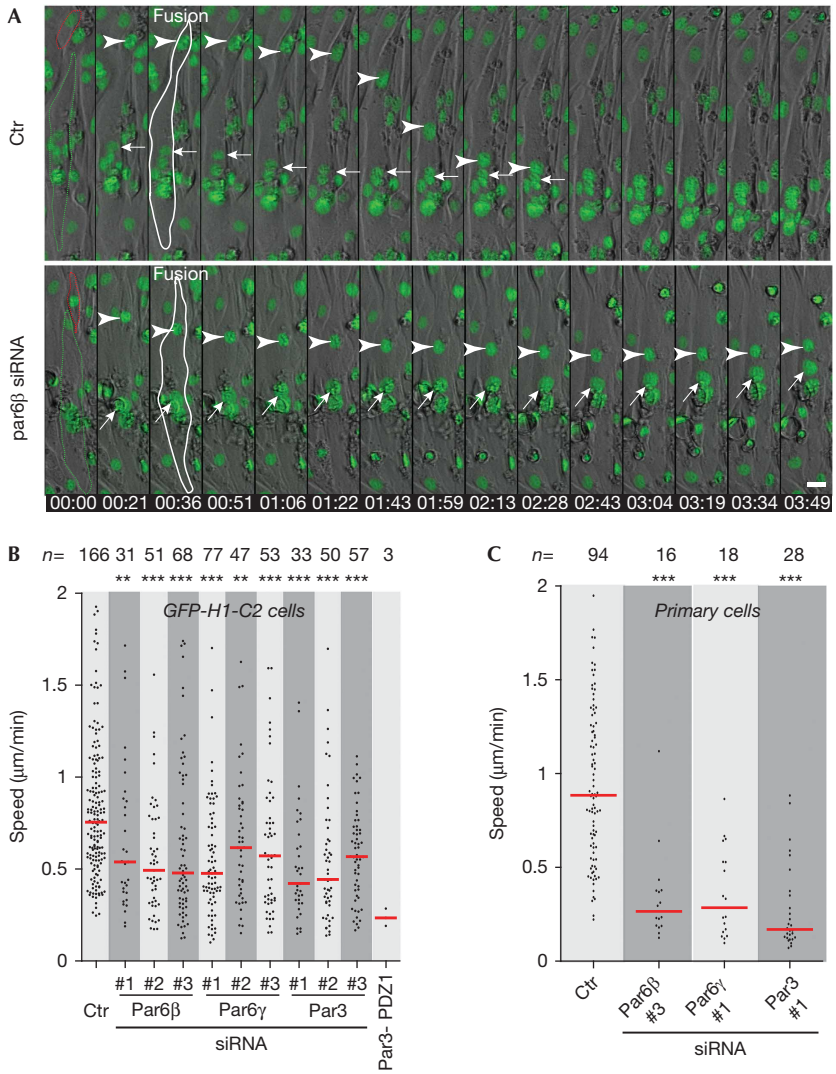

Fig 3 | Par proteins and dynein/dynactin complex are involved in nuclear movement after fusion. (**A**) Frames from a time-lapse two-channel movie (phase contrast and fluorescence) of differentiated GFP-H1-C2 cells untreated or Par6β siRNA treated annotated as in Fig 1A (supplementary Movie S7 online). Scale Bar, 20 μm. (**B**) Speed of the nuclei after fusion of differentiated GFP-H1-C2 cells nontreated, treated with three different siRNA against Par6β, Par6γ, Par3 or myotubes microinjected with YFP-Par3-PDZ1. (**C**) Speed of the nuclei after fusion of differentiated primary myoblasts in untreated or after transfection with the indicated siRNAs. *P*-value in (**B**,**C**); $^{**}P<0.01$, $^{***}P<0.005$. Red line indicates the median. GFP, green fluorescent protein; siRNA, short interfering RNA.

Par6β, Par6γ and Par3 with siRNA induced a significant reduction of nuclear movement after fusion, whereas Par6α siRNA did not have effect, in both GFP-H1-C2 and primary cells (Fig 3A–C; supplementary Fig S3a online, supplementary Movie S9 online). Efficiency and specificity of siRNA depletion were evaluated by western blot and reverse transcriptase PCR (supplementary Fig S2a,e–j online). No changes in fusion index were observed after siRNA transfection, with the exception of Par6γ siRNA where the fusion index was 60% of the control (supplementary Fig S1d online). MT organization was not affected under these conditions (supplementary Fig S5a,b online). Moreover, microinjection of myotubes with a dominant-negative construct of Par3 that disrupts Par3–Par6 interaction [26] also reduced nuclear movement after fusion (Fig 3B; supplementary Fig S3b online, supplementary Movie S10 online). Together, our results show that Par6 and Par3 control nuclear movement after fusion.

Par6b and dynactin accumulate at the NE

To understand how Par6 and dynein/dynactin complex are involved in nuclear movement after fusion, we determined their intracellular localization and found that Par6β, p50 and p150 accumulated at the NE of myotubes and differentiated myoblasts nuclei (which accumulate pericentrin at the NE; Figs 4A–E and 5E). In nondifferentiated myoblasts, Par6β was not at the NE whereas p50 and p150 were found at the centrosome (Fig 4C–E). These accumulations were significantly reduced in Par6β and p150 siRNA-treated cells (Fig 5A,C).

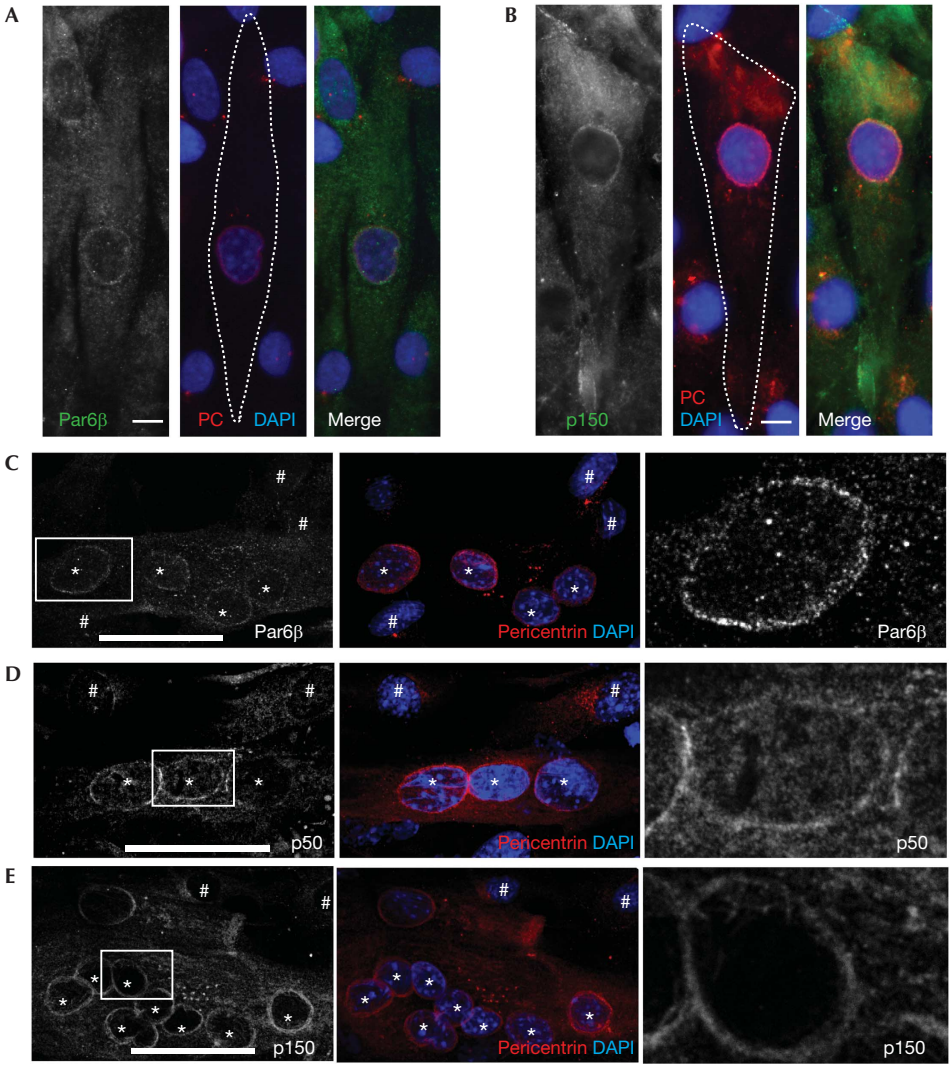

Fig 4 | Par6 and dynactin accumulate at the NE of differentiated myoblasts and myotubes. (**A**) Representative epi-fluorescence images of differentiated C2C12 myoblasts immunostained for Par6β, PC and DNA (DAPI). (**B**) Representative epi-fluorescence images of differentiated C2C12 myoblasts immunostained for p150, PC and DNA (DAPI). (**C–E**) Representative confocal images of differentiated C2C12 myotubes immunostained for Par6β (**C**), p50 (**D**) or p150 (**E**), pericentrin and DAPI. White square in left panel delineates the region showed in the right panel. Nondifferentiated myoblasts (#) and myotubes (*) nuclei are indicated based on pericentrin localization. Scale bars, 10 μm. NE, nuclear envelope; PC, pericentrin.

Fig 5 | Par proteins regulate Par6 and dynactin localization at the NE of differentiated myoblasts and myotubes. (**A**) Quantification of nuclei with Par6β ▶ at the NE in differentiated myoblasts and myotubes transfected with the indicated siRNAs, relative to non-siRNA control. At least 1,700 nuclei were counted corresponding to three independent experiments. (**B**) Representative epi-fluorescence images showing Par6β, pericentrin and DNA (DAPI) staining in control, Par6γ and DHC siRNA. (**C**) Quantification of nuclei with p150 at the NE in differentiated myoblasts and myotubes transfected with the indicated siRNAs, relative to non-siRNA control. At least 1,600 nuclei were counted corresponding to three independent experiments. (**D**) Representative epi-fluorescence images showing p150, pericentrin and DNA (DAPI) staining in control, Par6β and DHC siRNA. (**E**) Quantification of nuclei with Par6β and p150 at the NE of differentiated myoblasts and myotubes in cells untreated (Ctr) or treated with 5 μm nocodazole during 2 h before fixation (Ndz). At least 800 nuclei were counted corresponding to three independent experiments. (**F**) Proposed model for nuclear movement after fusion. Before fusion, both MTs from differentiated myoblast (orange) and myotube (green) nuclei are anchored by their minus ends to the nuclei with Par6β and dynein/dynactin at the NE (brown). After fusion, MTs emanating from the myoblast nucleus contact the nuclei of the myotube (green; left inset) and can be pulled by dynein/dynactin resulting in the movement of the myoblast nucleus towards the centre of the myotube (orange arrow). In addition, or in alternative, MTs emanating from the myotube nuclei might also contact the myoblast nuclei (orange; right inset) via dynein/dynactin resulting in the movement of the myoblast nucleus on the MTs. *P*-value in (**A**), (**C**) and (**E**); $*P<0.05$, $**P<0.01$. Errors bars are s.e.m. Scale bars, 10 μm. DHC, dynein heavy chain; MTs, microtubules; NE, nuclear envelope; siRNA, short interfering RNA.

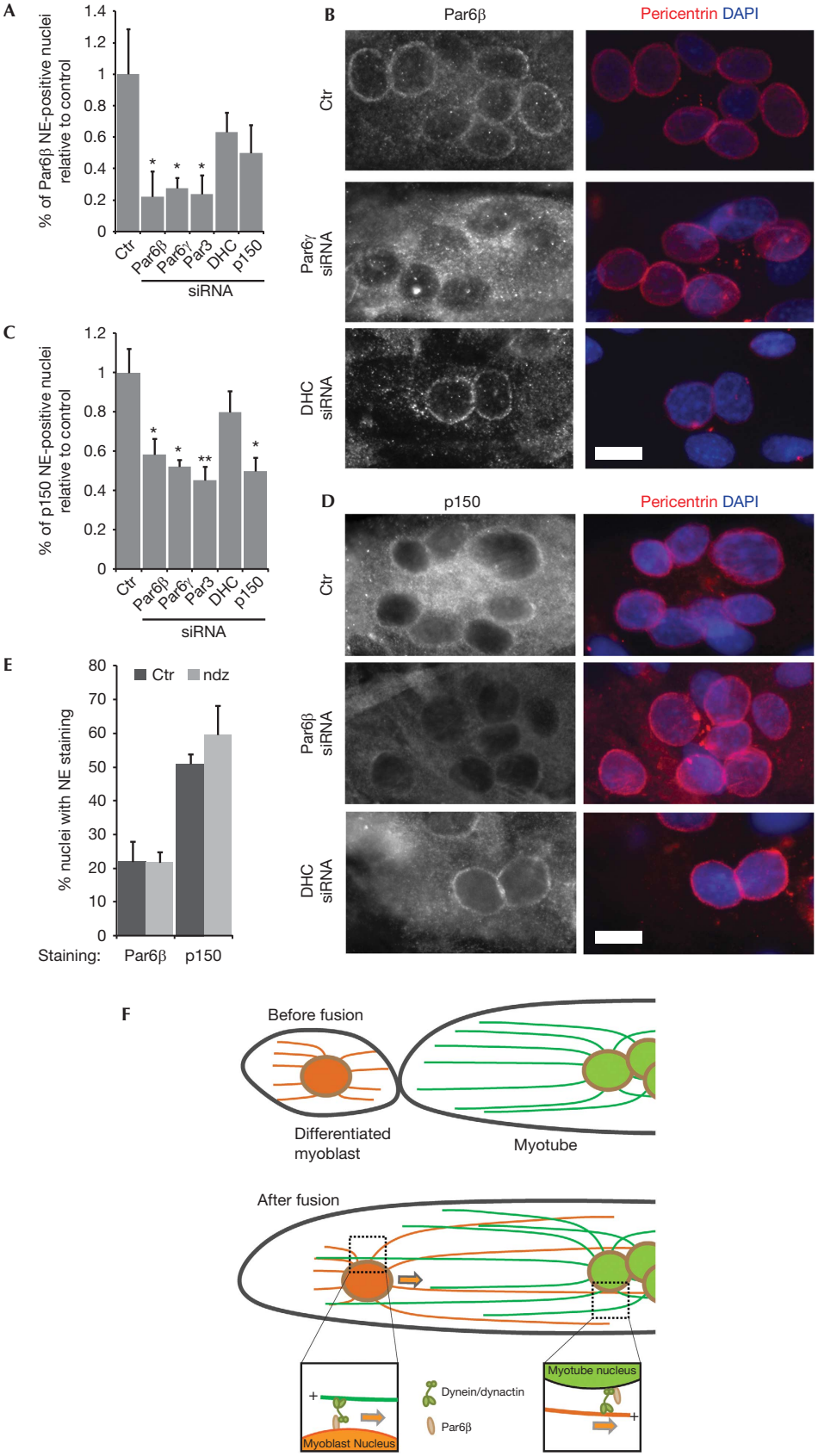
A
% of Par6β NE-positive nuclei relative to control
1.4
1.2
1
0.8
0.6
0.4
0.2
0
Ctr
Par6β
Par6γ
Par3
DHC
p150
siRNA
B
Par6β
Pericentrin DAPI
Ctr
Par6γ siRNA
DHC siRNA
C
% of p150 NE-positive nuclei relative to control
1.2
1
0.8
0.6
0.4
0.2
0
Ctr
Par6β
Par6γ
Par3
DHC
p150
siRNA
D
p150
Pericentrin DAPI
Ctr
Par6β siRNA
DHC siRNA
E
% nuclei with NE staining
80
70
60
50
40
30
20
10
0
Ctr
ndz
Staining:
Par6β
p150
F
Before fusion
Differentiated myoblast
Myotube
After fusion
Myoblast Nucleus
Dynein/dynactin
Par6β
Myotube nucleus

We then investigated how Par6β and p150 are recruited to the NE. Par6β NE accumulation was reduced by Par6γ and Par3 siRNA to the same extent as Par6β siRNA, whereas depletion of DHC or p150 had a lower effect (Fig 5A,B). Moreover, p150 NE accumulation was reduced by Par6β, Par6γ and Par3 siRNA to the same levels of p150 siRNA, whereas DHC siRNA had a lower effect (Fig 5C,D). Finally, we found that depolymerization of MTs did not disrupt the NE accumulation of Par6β and p150 (Fig 5E; supplementary Fig S4a–c online), thus MTs are not required for the localization of Par6β and p150 at the NE. These results suggest that Par6β, Par6γ and Par3 proteins are involved in the recruitment of dynein/dynactin complex to the NE, a new function for Par proteins and an alternative mechanism for the recruitment of dynein/dynactin complex to the NE [2,28–30]. Surprisingly, we also found that Par6β requires Par6γ for its proper localization to the NE. This indicates that there exists an as yet unappreciated cross dependence between Par6 proteins, and strongly suggests that these proteins may have different roles.

Overall, our results support a mechanism for nuclear movement after fusion where MTs emanating from the newly fused myoblast nucleus grow and reach the myotube nuclei in the centre of the myotube. Then, dynein/dynactin complex at the NE of myotube nuclei pulls on these MTs resulting in the movement of the myoblast nucleus from the periphery towards the centre of the myotube (Fig 5F). In alternative, dynein/dynactin complex at the NE of the newly fused myoblast nucleus can interact and move on MTs emanating from the myotube nuclei at the centre of the myotube (Fig 5F), as observed during zygote formation [3]. Our results do not discriminate between these two possibilities and both these mechanisms can simultaneously drive nuclear movement. The nuclear positioning events and mechanisms that we described are probably involved in muscle regeneration and misregulated in muscle pathologies. Future studies addressing this possibility will be important for understanding the processes of tissue regeneration and muscle pathologies.

METHODS

Myotube differentiation and fusion index. GFP-H1-C2 cells were plated on 0.1% gelatin-coated dishes or acid-washed coverslips for 1–2 days before differentiation. Primary myoblasts were plated on Matrigel (BD Biosciences)-coated dishes in 20% FBS IMDM supplemented with gentamycin at 0.05 mg/ml for 4 days before differentiation. Differentiation was induced by switching to DM (DMEM for C2C12 cells or IMDM for primary cells, with 1% horse serum). Fusion index was calculated as the percentage of nuclei inside myotubes with more than three nuclei relative to the total number of nuclei, and normalized relative to control conditions.

Microscopy. Epi-fluorescence images were acquired using a Nikon Ti microscope equipped with a CoolSNAP HQ2 camera (Roper Scientific), an XY-motorized stage (Nikon), using a ×40 1.0 NA PL APO oil or a ×100 1.4 NA PL APO oil objectives, driven by Metamorph (Molecular Devices). Multipositioning images were stitched with Metamorph (Molecular Devices). Life imaging was performed using an incubator to maintain cultures at 37 °C and 5% CO2 (Okolab) and ×10 0.3 NA PL Fluo dry or ×4 objectives. Confocal images were acquired using Leica SPE confocal microscope with a ×63 1.3 NA Apo objective.

Quantification of nuclear movement after fusion speed. Nuclear speed after fusion was measured in 60-h time-lapse movies acquired 2 days after switching to DM. Fusion events between myoblast and myotubes were identified by observation of time-lapse sequences. The position of the nucleus of the myoblast was manually determined for each frame after fusion using Metamorph (Molecular Devices), until the nucleus reached the cluster or up to 4 h after fusion. Nuclear movements were only measured in situations where the fusion event occurred more than 30 µm away from the myotube nuclei (distal end fusion). Nuclear movement speeds between consecutive frames were then calculated and averaged using Excel (Microsoft). Gaussian distribution of averaged speeds of each nuclei was tested using the D'Agostino and Pearson omnibus normality test for each conditions (GraphPad software); it appeared that the distribution was not Gaussian so the statistical significance between conditions was measured using the Mann–Whitney test for non-Gaussian distributions.

Supplementary information is available at EMBO *reports* online (http://www.emboreports.org).

ACKNOWLEDGEMENTS

We thank D. Sassoon, F. Relaix, M. Baylies, E. Folker, P. Tran, A. Merdes and A. Palazzo for comments on the manuscript. We thank the Gomes lab for discussions. B.C. was supported initially by a Fondation pour la Recherche Médicale (FRM) fellowship. V.G. was supported initially by a Region Ile-de-France fellowship. This work was supported by Muscular Dystrophy Association (MDA), INSERM Avenir programme and Agence Nationale de la Recherche (ANR) grants to E.R.G.

Author contributions: B.C., V.G. and E.R.G. conceived, designed and analysed the experiments. S.F. provided the primary muscle cells; and E.V. and C.B. provided Cdc42-lox primary muscle cells. B.C. and V.G. conducted the experimental work. The manuscript was written by B.C., V.G. and E.R.G. with assistance from other authors. Request for materials or reprints should be addressed to E.R.G.

CONFLICT OF INTEREST

The authors declare that they have no conflict of interest.

REFERENCES

1. Dauer WT, Worman HJ (2009) The Nuclear envelope as a signaling node in development and disease. *Dev Cell* **17:** 626–638
2. Starr DA, Fridolfsson HN (2010) Interactions between nuclei and the cytoskeleton are mediated by SUN-KASH nuclear-envelope bridges. *Annu Rev Cell Dev Biol* **26:** 421–444
3. Reinsch S, Gönczy P (1998) Mechanisms of nuclear positioning. *J Cell Sci* **111:** 2283–2295
4. Gomes ER, Jani S, Gundersen GG (2005) Nuclear movement regulated by Cdc42, MRCK, myosin, and actin flow establishes MTOC polarization in migrating cells. *Cell* **121:** 451–463
5. Cappello S *et al* (2006) The Rho-GTPase cdc42 regulates neural progenitor fate at the apical surface. *Nat Neurosci* **9:** 1099–1107
6. Joberty G, Petersen C, Gao L, Macara IG (2000) The cell-polarity protein Par6 links Par3 and atypical protein kinase C to Cdc42. *Nat Cell Biol* **2:** 531–539
7. Petronczki M, Knoblich JA (2001) DmPAR-6 directs epithelial polarity and asymmetric cell division of neuroblasts in Drosophila. *Nat Cell Biol* **3:** 43–49
8. Shi S-H, Jan LY, Jan Y-N (2003) Hippocampal neuronal polarity specified by spatially localized mPar3/mPar6 and PI 3-kinase activity. *Cell* **112:** 63–75
9. Doerflinger H, Vogt N, Torres IL, Mirouse V, Koch I, Nüsslein-Volhard C, St Johnston D (2010) Bazooka is required for polarisation of the Drosophila anterior-posterior axis. *Development* **137:** 1765–1773
10. Engel AG, Franzini-Armstrong C (1994) *Myology*. McGraw-Hill Professional Publishing: New York, New York, USA
11. Englander LL, Rubin LL (1987) Acetylcholine receptor clustering and nuclear movement in muscle fibers in culture. *J Cell Biol* **104:** 87–95

12. Dubowitz V, Sewry CA (2007) *Muscle Biopsy: A Practical Approach*. Saunders Elsevier: London, UK
13. Metzger T, Gache V, Xu M, Cadot B, Folker ES, Richardson BE, Gomes ER, Baylies MK (2012) MAP and kinesin-dependent nuclear positioning is required for skeletal muscle function. *Nature* **484:** 120–124
14. Tassin AM, Maro B, Bornens M (1985) Fate of microtubule-organizing centers during myogenesis *in vitro*. *J Cell Biol* **100:** 35–46
15. Warren RH (1974) Microtubular organization in elongating myogenic cells. *J Cell Biol* **63**(2 Pt 1): 550–566
16. Srsen V, Fant X, Heald R, Rabouille C, Merdes A (2009) Centrosome proteins form an insoluble perinuclear matrix during muscle cell differentiation. *BMC Cell Biol* **10:** 28
17. White SR, Evans KJ, Lary J, Cole JL, Lauring B (2007) Recognition of C-terminal amino acids in tubulin by pore loops in Spastin is important for microtubule severing. *J Cell Biol* **176:** 995–1005
18. Schiff PB, Horwitz SB (1980) Taxol stabilizes microtubules in mouse fibroblast cells. *Proc Natl Acad Sci USA* **77:** 1561–1565
19. Vasquez R, Howell B, Yvon A, Wadsworth P, Cassimeris L (1997) Nanomolar concentrations of nocodazole alter microtubule dynamic instability *in vivo* and *in vitro*. *Mol Biol Cell* **8:** 973–985
20. Gönczy P, Pichler S, Kirkham M, Hyman AA (1999) Cytoplasmic dynein is required for distinct aspects of MTOC positioning, including centrosome separation, in the one cell stage *Caenorhabditis elegans* embryo. *J.Cell Biol* **147:** 135–150
21. Burakov A, Nadezhdina E, Slepchenko B, Rodionov V (2003) Centrosome positioning in interphase cells. *J Cell Biol* **162:** 963–969
22. Meriane M, Roux P, Primig M, Fort P, Gauthier-Rouviere C (2000) Critical activities of Rac1 and Cdc42Hs in skeletal myogenesis: antagonistic effects of JNK and p38 pathways. *Mol Biol Cell* **11:** 2513–2528
23. Vasyutina E, Martarelli B, Brakebusch C, Wende H, Birchmeier C (2009) The small G-proteins Rac1 and Cdc42 are essential for myoblast fusion in the mouse. *Proc Natl Acad Sci USA* **106:** 8935–8940
24. Heasman SJ, Ridley AJ (2008) Mammalian Rho GTPases: new insights into their functions from *in vivo* studies. *Nat Rev Mol Cell Biol* **9:** 690–701
25. Etienne-Manneville S, Hall A (2001) Integrin-mediated activation of Cdc42 controls cell polarity in migrating astrocytes through PKCzeta. *Cell* **106:** 489–498
26. Schmoranzer J, Fawcett JP, Segura M, Tan S, Vallee RB, Pawson T, Gundersen GG (2009) Par3 and dynein associate to regulate local microtubule dynamics and centrosome orientation during migration. *Curr Biol* **19:** 1065–1074
27. Gao L, Macara IG (2004) Isoforms of the polarity protein Par6 have distinct functions. *J Biol Chem* **279:** 41557–41562
28. Salina D, Bodoor K, Eckley D, Schroer T, Rattner JB, Burke B (2002) Cytoplasmic dynein as a facilitator of nuclear envelope breakdown. *Cell* **108:** 97–107
29. Bolhy S, Bouhlel I, Dultz E, Nayak T, Zuccolo M, Gatti X, Vallee R, Ellenberg J, Doye V (2011) A Nup133-dependent NPC-anchored network tethers centrosomes to the nuclear envelope in prophase. *J Cell Biol* **192:** 855–871
30. Splinter D *et al* (2010) Bicaudal D2, dynein, and kinesin-1 associate with nuclear pore complexes and regulate centrosome and nuclear positioning during mitotic entry. *PLoS Biol* **8:** e1000350